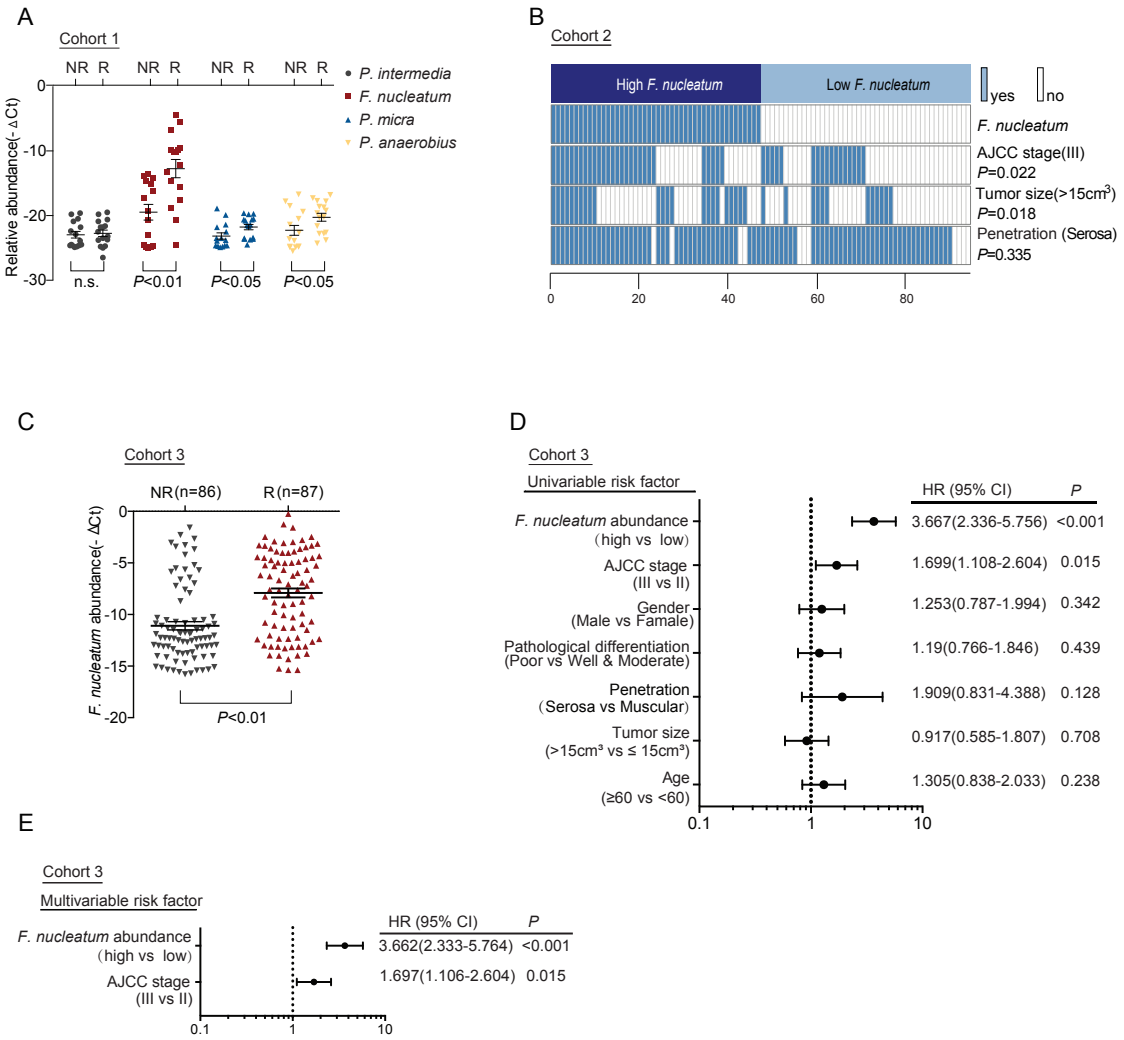

Figure S1. *F. nucleatum* Is Associated with Cancer Recurrence and Patient Outcome, Related to Figure 1

(A) Statistical analysis of *P. intermedia, F. nucleatum, P. micra, P. anaerobius* amounts in CRC tissues from patients without recurrence (n = 15) and with recurrence (n = 16), nonparametric Mann–Whitney test. The bars represent SE.

(B) Comparing tumor size, positive or negative serosal invasion, and AJCC stage between *F. nucleatum* high-expression and low-expression tumors of Cohort 2. The heatmap illustrates the association of different clinical characters with *F. nucleatum* high- and low-expression tumors. Statistical significance was performed by Chi-square test.

(C) Statistical analysis of *F. nucleatum* amount in CRC tissues from patients without recurrence (n = 86) and with recurrence (n = 87) (Cohort 3), nonparametric Mann–Whitney test. The bars represent SE.

(D) Univariate analysis was performed in the Cohort 3. The bars correspond to 95% confidence intervals.

(E) Multivariate analysis was performed in the Cohort 3. The bars correspond to 95% confidence intervals. NR, non-recurrence; R, recurrence.

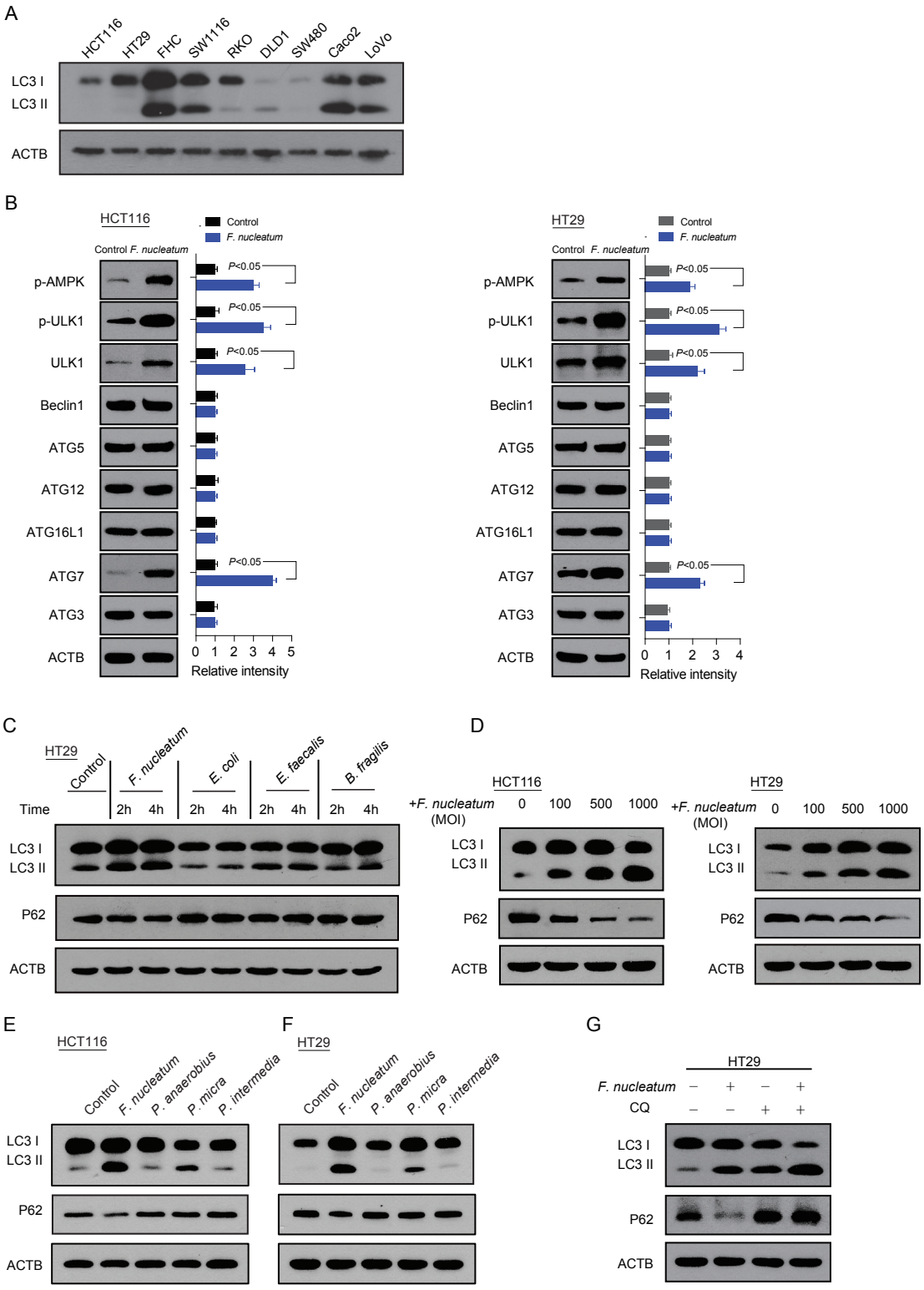

Figure S2. *F. nucleatum* Promotes Cancer Autophagy Activation, Related to Figure 2

(A) The basic levels of LC3 protein in nine colorectal epithelial cell lines were detected by western blot assays.

(B) Western blot was performed to detect autophagy-related protein expression in HCT116 cells (left) and HT29 cells (right) co-cultured with *F. nucleatum*, nonparametric Mann–Whitney test. The relative density of each band was analyzed by ImageJ software.

(legend continued on next page)

(C) Western blot was used to detect LC-3I, LC-3II, and p62 expression in HT29 cells co-cultured with *F. nucleatum*, or *E. coli,* or *E. faecalis*, or *B. fragilis*, respectively.
(D) Western blot was used to detect LC-3I, LC-3II, and p62 expression in HCT116 cells (left) and HT29 (right) cells co-cultured with *F. nucleatum* at different multiplicity of infection (MOI).
(E and F) Western blot was used to detect LC-3I and LC-3II expression in HCT116 cells (E) and HT29 cells (F) co-cultured with *F. nucleatum*, *P. anaerobius*, *P. micra or P. intermedia*, respectively.
(G) Western blot was performed to detect LC-3I, LC-3II, and p62 expression in HT29 cells co-cultured with *F. nucleatum* and CQ.

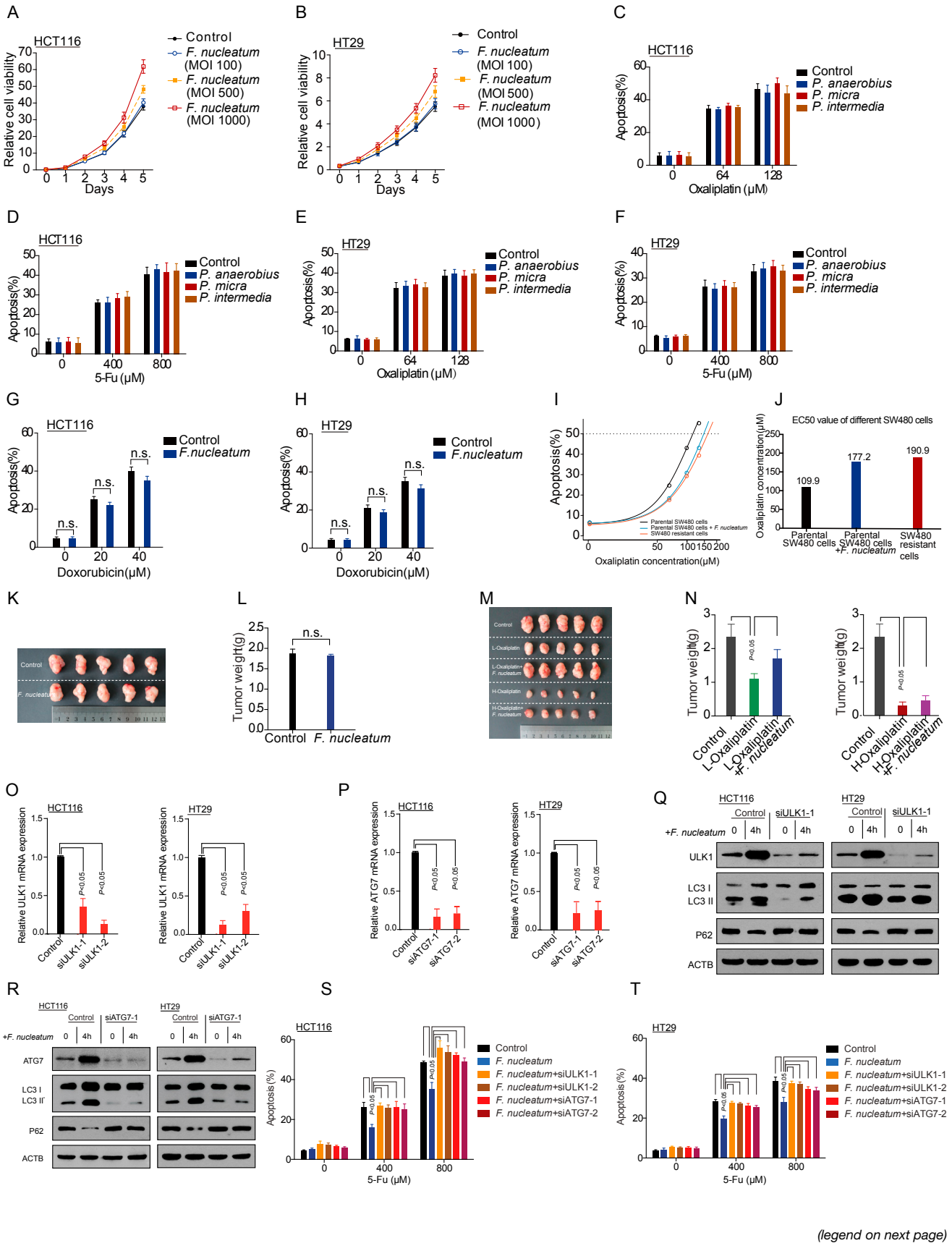

(legend on next page)

Figure S3. *F. nucleatum* Induces Chemoresistance in Colorectal Cancer Cells via Activation of the Autophagy Pathway, Related to Figure 3

(A and B) Cell proliferation was detected in HCT116 cells (A) and HT29 cells (B) co-cultured with *F. nucleatum* at different MOIs, non-parametric Mann-Whitney test.

(C–F) Apoptosis was detected by flow cytometry in HCT116 cells (C, D) and HT29 cells (E, F). The cells were independently co-cultured with *F. nucleatum*, *P. anaerobius*, *P. micra, or P. intermedia* and treated with different concentrations of Oxaliplatin (C, E) and 5-Fu (D, F), nonparametric Mann–Whitney test.

(G and H) Apoptosis was detected by flow cytometry in HCT116 cells (G) and HT29 cells (H). The cells were co-cultured with *F. nucleatum* and treated with different concentrations of Doxorubicin, nonparametric Mann–Whitney test.

(I) Apoptosis was detected by flow cytometry in parental SW480 cells, Oxaliplatin-resistant SW480 cells, and parental SW480 cells co-cultured with *F. nucleatum* in the presence of different concentrations of Oxaliplatin. Each point is the mean of 3 replicates. All analyses were performed using R software using the Analysis of Dose-Response Curves (DRC) package.

(J) The EC_{50} value in different SW480 cells treated with Oxaliplatin.

(K–N) Representative data of tumors in nude mice bearing SW480 cells in different experimental conditions (K, M). Statistical analysis of mouse tumor weights in different groups **(L, N)**, n = 8/group, nonparametric Mann–Whitney test. L-Oxaliplatin, low concentration of Oxaliplatin; H-Oxaliplatin, high concentration of Oxaliplatin.

(O) Real-time PCR was performed to detect *ULK1* mRNA level in HCT116 cells (left) and HT29 cells (right) transfected with ULK1 siRNAs. n = 3, non-parametric Mann-Whitney test.

(P) Real-time PCR was performed to detect *ATG7* mRNA level in HCT116 cells (left) and HT29 cells (right) cells transfected with ATG7 siRNAs. n = 3, non-parametric Mann-Whitney test.

(Q) Western blot was performed to detect ULK1, LC-3I, LC-3II, and p62 expression in HCT116 cells (left) and HT29 cells (right) transfected with ULK1 siRNA-1 and co-cultured with *F. nucleatum*.

(R) Western blot was performed to detect ATG7, LC-3I, LC-3II, and p62 expression in HCT116 cells (left) and HT29 cells (right) transfected with ATG7 siRNA-1 and co-cultured with *F. nucleatum*.

(S and T) Apoptosis was detected by flow cytometry in HCT116 cells (S) and HT29 cells (T). The cells were co-cultured with *F. nucleatum* after ULK1 and ATG7 siRNAs transfection and subsequently treated with different concentrations of 5-Fu, nonparametric Mann–Whitney test.

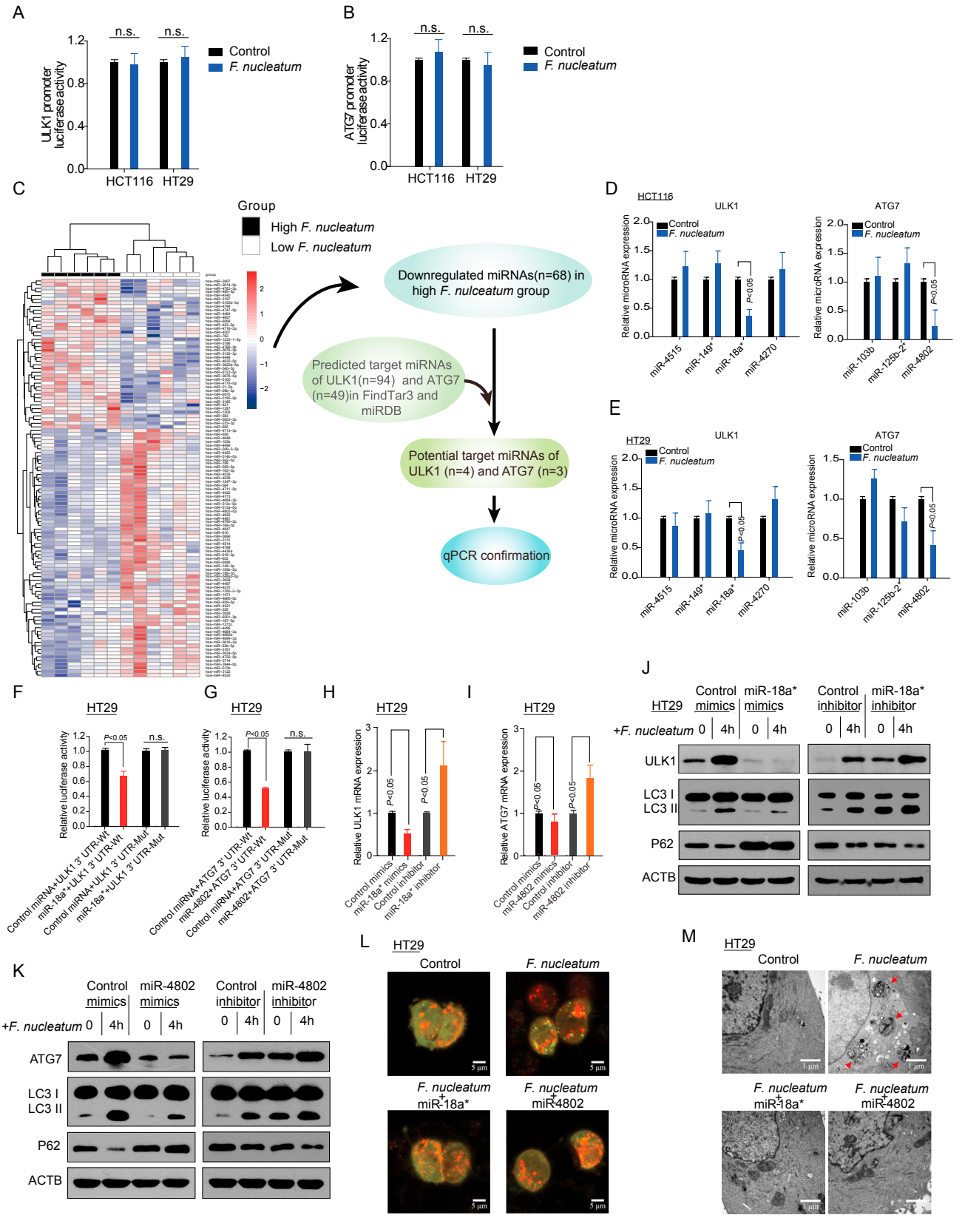

(legend on next page)

Figure S4. *F. nucleatum* Activates Cancer Autophagy via Downregulation of miR-18a* and miR-4802, Related to Figure 4

(A and B) Luciferase assays were performed in HCT116 and HT29 cells. The cells were co-cultured with *F. nucleatum* after transfection of *ULK1* (**A**) and *ATG7* (**B**) promoter plasmids. n.s., not significant.

(C) Six pairs of CRC tissues were chosen for miRNA Chip array (left). The abundance of *F. nucleatum* was used as the basis for grouping, n = 6. Schematic of target miRNA candidate screening process is shown (right).

(D and E) Expression of candidate miRNAs was quantified by real-time PCR in HCT116 cells (D) and HT29 cells (E). n = 3.

(F and G) Luciferase activity was measured in HT29 cells. The luciferase reporters expressing wild-type or mutant human *ULK1* 3′UTRs (F) and *ATG7* 3′UTRs (G) were used. The cells were co-transfected with miR-18a* mimics, miR-4802 mimics, or control miRNA.

(H and I) Real-time PCR was performed in HT29 cells to detect the expression of *ULK1* (H) and *ATG7* (I) genes. The cells were transfected with miR-18a* mimics, miR-4802 mimics, or inhibitor, nonparametric Mann–Whitney test.

(J and K) Autophagy-related proteins were detected by western blot in HT29 cells. The cells were transfected with mimics or inhibitor of miR-18a* (J) and miR-4802 (K), then co-cultured with *F. nucleatum.*

(L) Autophagosomes were detected with confocal microscope (2000 × magnification) in HT29 cells. The cells expressing mRFP-GFP-LC3 fusion protein were transfected with miR-18a* (left) and miR-4802(right) mimics, then cultured with *F. nucleatum*, Bar scale, 5 μm.

(M) Autophagosomes were observed by transmission electron microscopy (17500 × magnification) in HT29 cells. The cells were transfected with miR-18a* (left) and miR-4802 (right) mimics, then co-cultured with *F. nucleatum.* Bar scale, 1 μm.

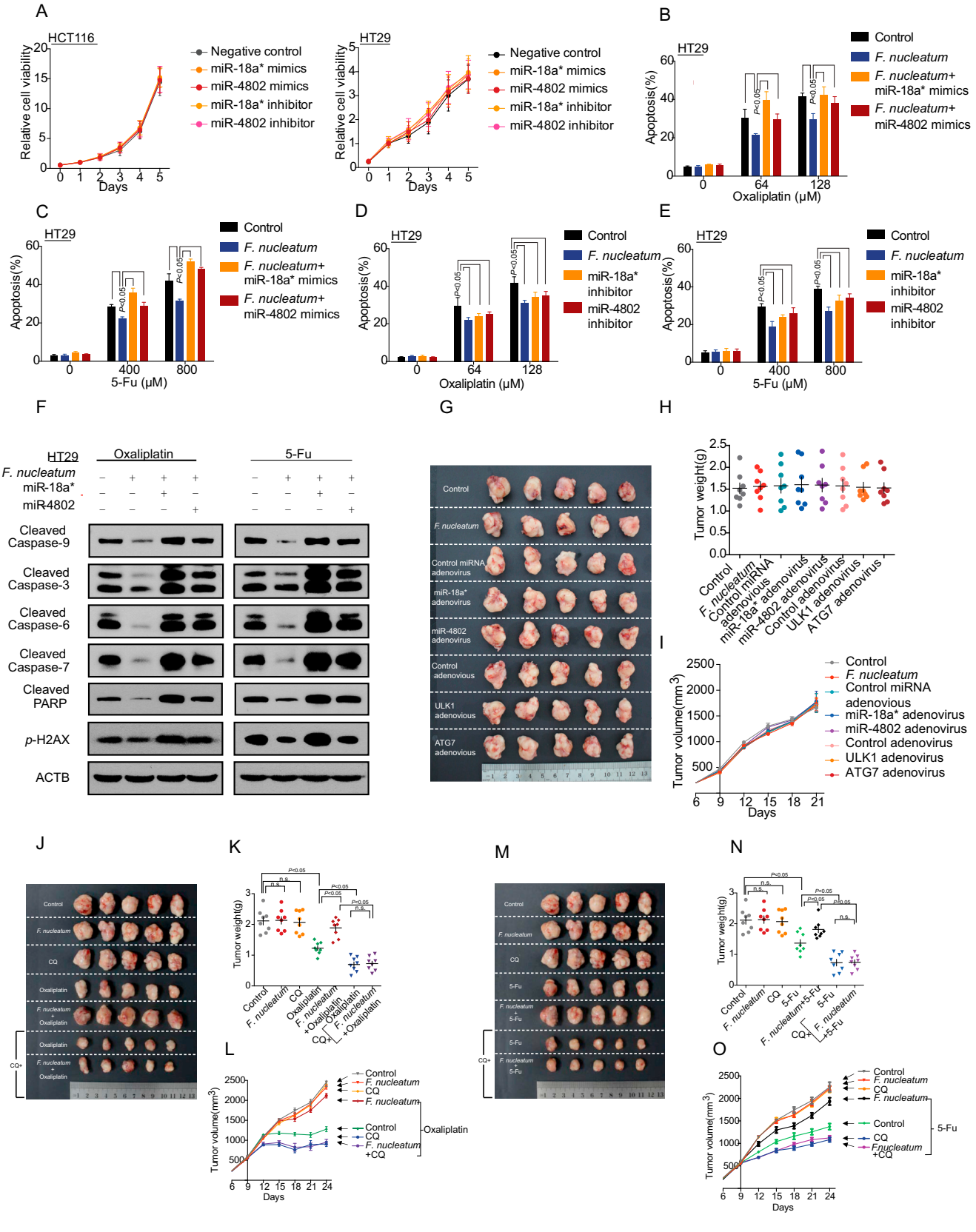

(legend on next page)

Figure S5. MiR-18a* and miR-4802 Regulate *F. nucleatum*-Mediated Chemoresistance, Related to Figure 5

(A) Cell proliferation was detected in HCT116 cells (left) and HT29 (right) cells after transfection with mimics or inhibitor of miR-18a* and miR-4802, non-parametric Mann-Whitney test.

(B–E) Apoptosis was detected by flow cytometry in HT29 cells. The cells were independently transfected with the mimics (B, C) or inhibitors (D, E) of miR-18a* and miR-4802, then co-cultured with *F. nucleatum*, and treated with different concentrations of Oxaliplatin (B, D) and 5-Fu (C, E). Nonparametric Mann–Whitney test.

(F) Western blot was performed to detect apoptosis-related protein levels in HT29 cells with different treatments. Oxaliplatin (left) or 5-Fu (right).

(G) Representative data of tumors in nude mice bearing colorectal cancer cells in eight control groups.

(H and I) Statistical analysis of mouse tumor weights (H) and volumes (I) in control groups, n = 8/group, nonparametric Mann–Whitney test.

(J) Representative data of tumors in nude mice bearing colorectal cancer cells in different groups.

(K–L) Statistical analysis of mouse tumor weights (K) and volumes (L) in different groups, n = 8/group, nonparametric Mann–Whitney test.

(M) Representative data of tumors in nude mice bearing colorectal cancer cells in different groups. (J) and (M) shared the experimental controls.

(N and O) Statistical analysis of mouse tumor weights (N) and volumes (O) in different groups, n = 8/group, nonparametric Mann–Whitney test.

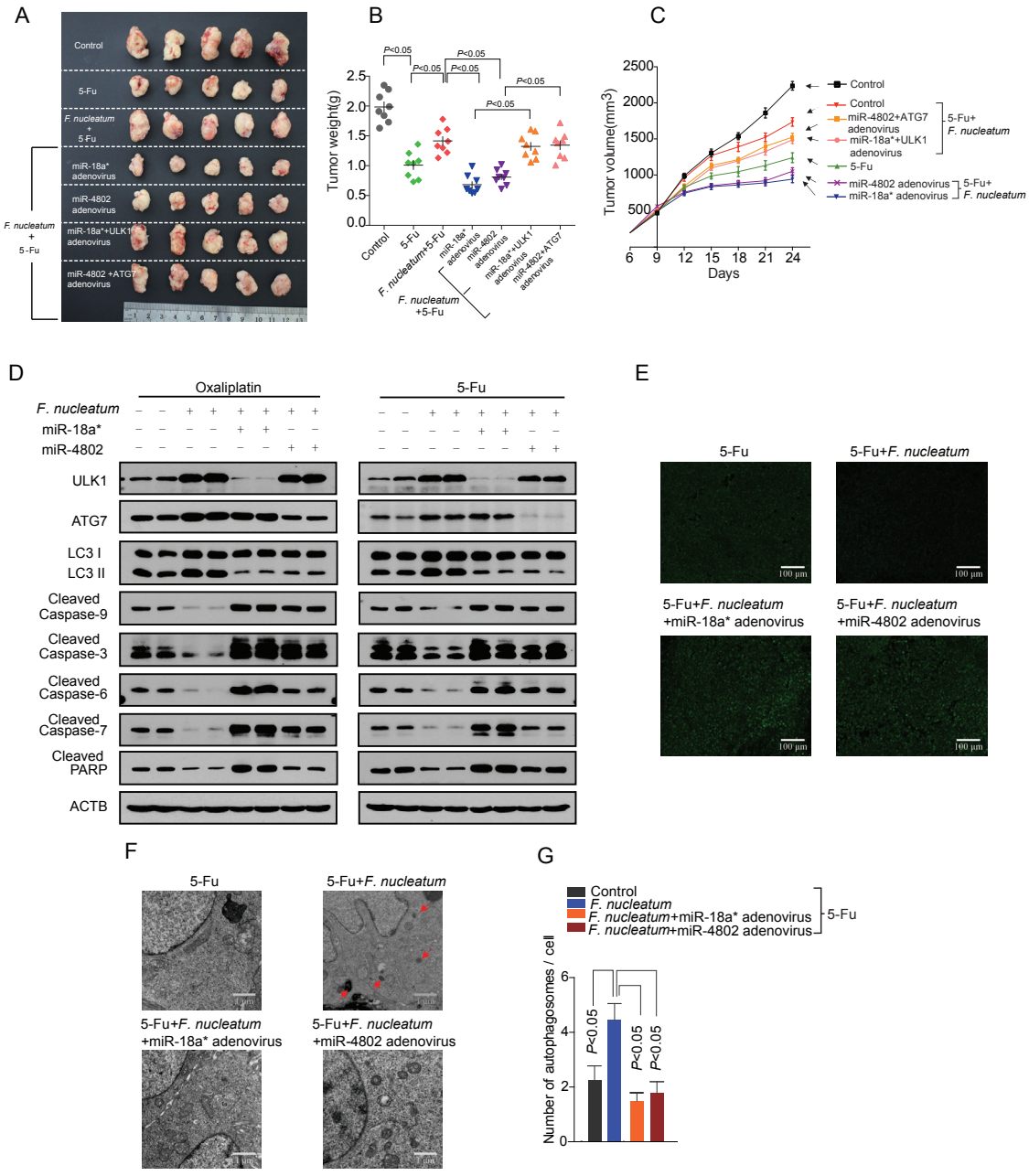

Figure S6. MiR-18a* and miR-4802 Regulate *F. nucleatum*-Mediated Chemoresistance In Vivo, Related to Figure 5

(A) Representative data of tumors in nude mice bearing colorectal cancer cells in different groups.

(B and C) Statistical analysis of mouse tumor weights (Q) and volumes (R) in different groups, n = 8/group, nonparametric Mann–Whitney test.

(D) Western blot was performed to detect autophagy and apoptosis-related proteins in xenograft tumors after different treatments.

(E) TUNEL assays were performed to detect the apoptosis in the xenograft tissues after 5-Fu and *F. nucleatum* treatment with or without miR-18a* and miR-4802 overexpression.

(F) Transmission electron microscopy was performed to detect autophagosomes in xenograft tissues after 5-Fu and *F. nucleatum* treatment with or without miR-18a* and miR-4802 overexpression (17500 × magnification). Bar scale, 1 μm.

(G) Statistical analysis of autophagosomes in the xenograft tissues detected by transmission electron microscopy, nonparametric Mann–Whitney test.

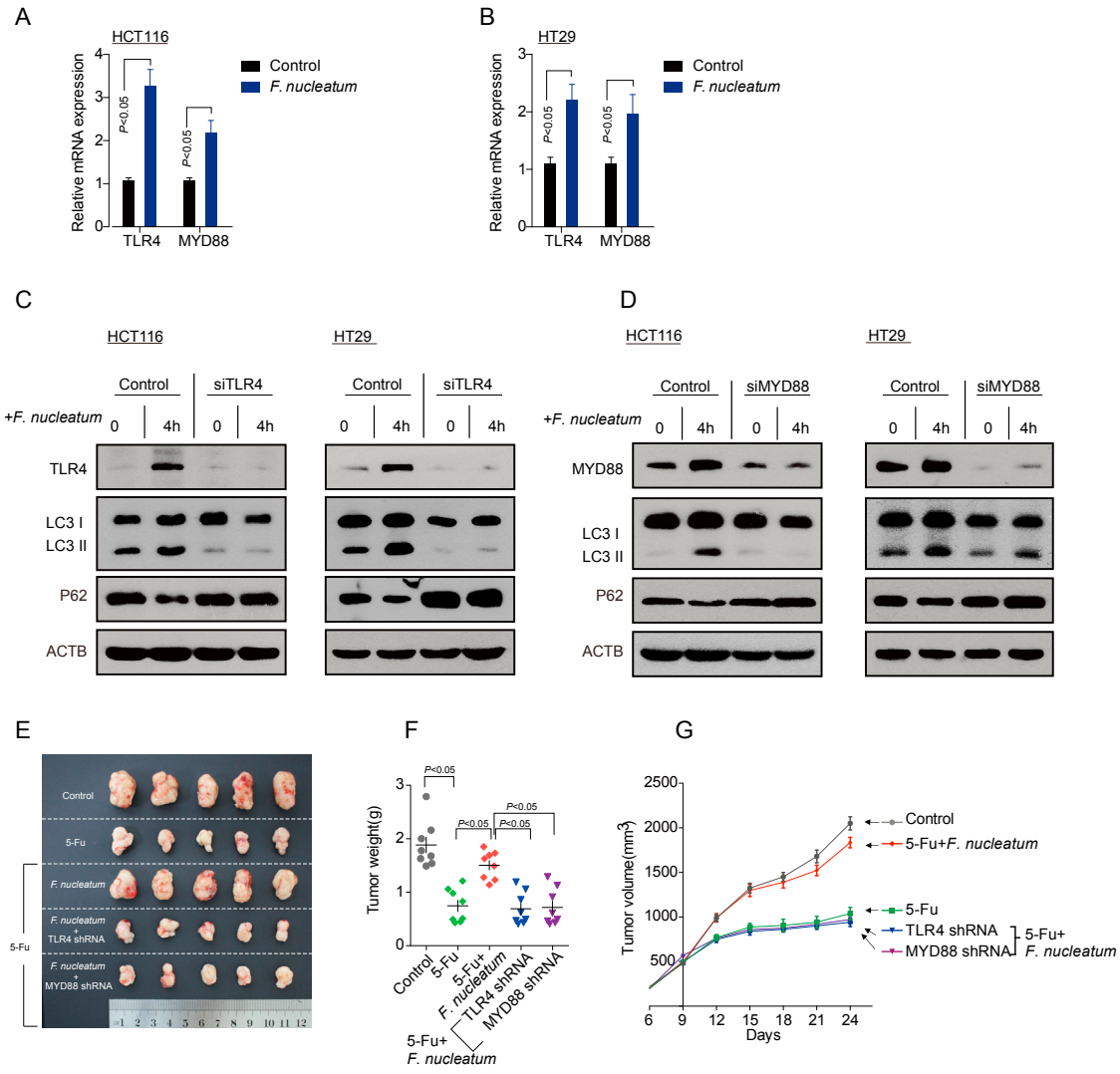

Figure S7. TLR4 and MYD88 Pathway Is Involved in *F. nucleatum*-Mediated Chemoresistance, Related to Figure 6

(A and B) Real-time PCR was performed in HCT116 cells (A) and HT29 cells (B) to detect the expression of *TLR4* and *MYD88* genes, the cells were co-cultured with *F. nucleatum*, nonparametric Mann–Whitney test.

(C) Western blot was performed in HCT116 cells (left) and HT29 cells (right). The cells were co-cultured with *F. nucleatum* and transfected with TLR4 siRNAs.

(D) Western blot was performed in HCT116 (left) and HT29 (right) cells. HT29 cells were co-cultured with *F. nucleatum* and transfected with MYD88 siRNAs.

(E) Representative data of tumors in nude mice bearing colorectal cancer cells in different groups.

(F and G) Statistical analysis of mice tumor weights (F) and volumes (G) in different groups, n = 8/group, nonparametric Mann–Whitney test.